Numerical Simulation of Tidal Current around Keelung Sill off Northern Taiwan

Hsien-Wen Li[1], Yao-Tsai Lo[2], Cheng-Han Tsai[2], Nan-Jung Kuo[2], Chung-Ru Ho[2], Dong-Jiing Doong[2], Shih-Jen Huang[2], Hung-Jen Lee[2] and Young-Zehr Kehr[3]

(1) Department of Civil Engineering and Environmental Informatics, Minghsin University of Science and Technology, 1 Hsin-Hsing Road, Hsin-Fong, Hsin-Chu County 30401, Taiwan (lihw@must.edu.tw)

(2) Department of Marine Environmental Informatics, National Taiwan Ocean University, Keelung, Taiwan

(3) Department of Systems Engineering and Naval Architecture, National Taiwan Ocean University, Keelung, Taiwan

***Abstract*-Tidal power is a renewable energy source and considered as one of energy solutions in the context of global warming. The Keelung Sill is a seamount-like formation with depths in the range of 10-40m on a 60m deep sea floor. It is located between the Keelung Island and the Keelung Harbor on the north coast of Taiwan. Due to its shallowness, currents measured at the Sill are often above 1.5 m/s and can be as high as 2.5 m/s. Since Keelung Sill is only about 3 km off the Keelung Harbor, it can be an ideal site for tidal power generation. In this study we have established a two-dimensional numerical model to simulate tidal currents around the Keelung Sill. The numerical model to be used is based on the hydrodynamic equations and constructed by the finite difference method. The model was mainly driven by tides from open boundaries, in which the tides are obtained from a global tidal model of Japan's National Astronomical Observatory (NAO). The model result indicated that the strongest current in a 24-hr cycle is about 1.0 m/s, which is lower than observed. It may be due to the lunar phase of simulation day different from the measurement time.**

I. INTRODUCTION

The Keelung Island is a very small island, which lies off the Keelung Harbor on the northern coast of Taiwan. The Keelung Sill is a narrow seamount-like formation which extends from the Keelung Island southward to the neighborhood of the Keelung Harbor. The tidal wave propagates from east to west along northern coast of Taiwan. When tidal wave passes the Keelung Sill between the Keelung Harbor and Keelung Island, the tidal currents will accelerate due to the shallow bottom topography. The speeds of tidal currents on the Keelung Sill are about 1.5m/s, and the strong tidal currents will be a renewable energy source of tidal power generator. This study is to develop a numerical model to simulate tidal current distribution and to find a most suitable site for constructing the tidal power generator. The principal concept to develop this model is the same as that is employed by one of the authors, as in [1] and [2].

II. GOVERNING EQUATIONS

The following system of hydrodynamic equations is used for development of a numerical model of tidal currents,

$$\frac{\partial U}{\partial t} = fV - g(\zeta + H)\frac{\partial \zeta}{\partial x} - \frac{T_{bx}}{\rho} - \left(\frac{\partial}{\partial x}\int_{-H}^{\zeta} uu\,dz + \frac{\partial}{\partial y}\int_{-H}^{\zeta} uv\,dz\right) + \frac{\partial}{\partial x}\int_{-H}^{\zeta} A\frac{\partial u}{\partial x}dz + \frac{\partial}{\partial y}\int_{-H}^{\zeta} A\frac{\partial u}{\partial y}dz \tag{1}$$

$$\frac{\partial V}{\partial t} = -fU - g(\zeta + H)\frac{\partial \zeta}{\partial y} - \frac{T_{by}}{\rho} - \left(\frac{\partial}{\partial x}\int_{-H}^{\zeta} vu\,dz + \frac{\partial}{\partial y}\int_{-H}^{\zeta} vv\,dz\right) + \frac{\partial}{\partial x}\int_{-H}^{\zeta} A\frac{\partial v}{\partial x}dz + \frac{\partial}{\partial y}\int_{-H}^{\zeta} A\frac{\partial v}{\partial y}dz \tag{2}$$

$$\frac{\partial \zeta}{\partial t} = -\left(\frac{\partial U}{\partial x} + \frac{\partial V}{\partial y}\right) \tag{3}$$

Here x, y, z are components of a Cartesian coordinate system, with x, y, z axes in eastward, northward and upward directions respectively. u and v are velocity components in x and y directions respectively; ρ is the density of seawater which is assumed here as a constant, g is the acceleration due to gravity and f the Coriolis parameter, and A is the horizontal eddy viscosity coefficient. The tide-generating forces are neglected because of the small area of this model. (U, V) is the volume transport vector. ζ is the free surface displacement from the undisturbed state and positive upward. T_{bx} and T_{by} are bottom stresses in x and y components, which are exerted by the sea water upon the sea bottom.

Equations (1) and (2) are vertical integration of the equations of motion in x and y components respectively. Equation (3) is vertical integration of the continuity equation for an incompressible fluid. In the procedure of vertical integration we have used the hydrostatic equation to determine the pressure at depth z and incorporated the corresponding boundary conditions of neglecting air pressure gradient.

A measure of water velocity is then obtained by averaging this volume transport over depth, thus

978-1-4244-5222-4/10/$26.00 ©2010 IEEE

$$\bar{u} = \frac{U}{\zeta + H}, \qquad \bar{v} = \frac{V}{\zeta + H}.$$

Because the surface displacement ζ is much smaller than the water depth H, we will take $(\zeta + H) = H$.

Assuming the horizontal eddy viscosity to be constant and the velocities to be uniform with the depth, the expressions for the turbulent friction of x-component can be approximated as follows,

$$\int_{-H}^{\zeta} A\frac{\partial u}{\partial x}dz = A\frac{\partial U}{\partial x} \quad , \quad \int_{-H}^{\zeta} A\frac{\partial u}{\partial y}dz = A\frac{\partial U}{\partial y}$$

The computation for y-component is similar as above. We also assumed a constant horizontal dynamic eddy viscosity coefficient, $A = 1.025 \times 102\ \mathrm{m^2/s}$ [3].

On assuming a uniform velocity distribution in the vertical, the bottom friction can be approximated as follows,

$$\frac{(T_{bx}, T_{by})}{\rho} = k\frac{(U,V)}{H}\frac{|(U,V)|}{H}$$

where k is a nondimensional skin friction coefficient of the order of 2.5×10^{-3} [3].

The nonlinear terms may be approximated as follows,

$$\int_{-H}^{\zeta} uu\,dz = \frac{UU}{H} \quad , \quad \int_{-H}^{\zeta} uv\,dz = \frac{UV}{H} \quad , \quad \int_{-H}^{\zeta} vv\,dz = \frac{VV}{H}$$

With the above approximations equations (1), (2), and (3) can be solved numerically by means of finite difference method. Here we use the conjugate lattice [4] for space-time-differencing.

The derivatives in time and space are approximated by the central difference scheme, where the divergence, the surface gradient and the Coriolis terms are evaluated at a time-step centered between the old and new time. The dissipation terms and nonlinear terms are evaluated at the old time step. The stability criterion is the familiar Courant-Friedrich-Lewy condition,

$$\frac{\Delta t}{\Delta s} < \frac{1/\sqrt{2}}{C_{\max}}$$

where $C_{\max}$ is the speed of propagation of the fastest waves in the model. Thus $C_{\max} = (gH_{\max})^{1/2}$, which is the fastest speed of shallow water wave, and $H_{\max}$ is the maximum depth in this area. The model domain is from 121.73° to 121.84° E and from 25.12° to 25.21° N, as shown in Fig, 1. Within this domain $H_{\max}$ is 150m. In this model $\Delta s (= \Delta x = \Delta y)$ equals to 50m. Therefore we choose $\Delta t = 0.9$s for calculation.

The equations (1), (2) and (3) are then approximated as follows [2],

$$\begin{aligned} U(x,y,t+\tfrac{1}{2}\Delta t) &= U(x,y,t-\tfrac{1}{2}\Delta t) + \frac{\Delta t}{2} f\left\{V(x,y,t-\tfrac{1}{2}\Delta t) + V(x,y,t+\tfrac{1}{2}\Delta t)\right\} \\ &- \frac{\Delta t}{\Delta x} gH\left\{\zeta(x+\tfrac{1}{2}\Delta x,y,t) - \zeta(x-\tfrac{1}{2}\Delta x,y,t)\right\} - \Delta t\left(\frac{T_{bx}}{\rho}\right) \\ &- \Delta t\left\{\frac{\partial(UU/H)}{\partial x} + \frac{\partial(UV/H)}{\partial y}\right\} + \Delta t\left\{A\left(\frac{\partial^2 U}{\partial x^2} + \frac{\partial^2 U}{\partial y^2}\right)\right\} \end{aligned} \quad (4)$$

$$\begin{aligned} V(x,y,t+\tfrac{1}{2}\Delta t) &= V(x,y,t-\tfrac{1}{2}\Delta t) - \frac{\Delta t}{2} f\left\{U(x,y,t-\tfrac{1}{2}\Delta t) + U(x,y,t+\tfrac{1}{2}\Delta t)\right\} \\ &- \frac{\Delta t}{\Delta y} gH\left\{\zeta(x,y+\tfrac{1}{2}\Delta y,t) - \zeta(x,y-\tfrac{1}{2}\Delta y,t)\right\} - \Delta t\left(\frac{T_{by}}{\rho}\right) \\ &- \Delta t\left\{\frac{\partial(VU/H)}{\partial x} + \frac{\partial(VV/H)}{\partial y}\right\} + \Delta t\left\{A\left(\frac{\partial^2 V}{\partial x^2} + \frac{\partial^2 V}{\partial y^2}\right)\right\} \end{aligned} \quad (5)$$

$$\begin{aligned} \zeta(x,y,t) &= \zeta(x,y,t-\Delta t) - \frac{\Delta t}{\Delta x}\left\{U(x+\tfrac{1}{2}\Delta x,y,t-\tfrac{1}{2}\Delta t) - U(x-\tfrac{1}{2}\Delta x,y,t-\tfrac{1}{2}\Delta t)\right\} \\ &- \frac{\Delta t}{\Delta y}\left\{V(x,y+\tfrac{1}{2}\Delta y,t-\tfrac{1}{2}\Delta t) - V(x,y-\tfrac{1}{2}\Delta y,t-\tfrac{1}{2}\Delta t)\right\} \end{aligned} \quad (6)$$

The lateral boundary points are composed of U and V points along the coastline, where the no-s1ip condition is used, i.e. $U = 0$, $V = 0$. The tidal heights calculated by means of Japan's NAO tide model [5] were substituted into the ζ points along the open boundaries.

III. Results and Discussion

We simulated the tidal currents over the Keelung Sill in a 24-hr tidal cycle. The results are shown in Fig. 2 for the first hour and Figs. 3-10 for every three hours. The insets in these figures show the time corresponding to the tidal height at the Keelung Harbor. The area in these figures is cut from the model domain to give a better view of tidal current distribution around Keelung Sill. The tidal currents flow westward as the tide rises, and flow eastward as it falls. The strongest current is at the time near high tide and low tide, and its speed is about 1.0 m/s. It is lower than the measured value. It may be due to the lunar phase of simulation day different from the measurement time.

IV. Conclusions

The Keeling Sill is nearly in the south-north direction, which is almost perpendicular to the predominant tidal currents. The simulation of tidal current shows the flow pattern in a 24-hr cycle in the area surrounding the Sill, and demonstrates the currents are strongest in the periods of flood and ebb tides over the Sill. The weak currents appear in the inflection of tidal height, which is only a short interval. We will do more computations for different lunar phases to better understand the tidal current pattern over the Sill.

ACKNOWLEDGMENT

This research is supported by the National Science Council of Taiwan, the Republic of China under contract NSC 98-3114-E-019-002.

REFERENCES

[1] Hsien-Wen Li, “A numerical predictive model of tides in the seas adjacent to Taiwan,” Proc. Natl. Sci. Counc. ROC(A), vol.11, no.1, pp. 74-89,January 1987.

[2] Hsien-Wen Li and Yung-Ching Wu, “A numerical predictive model of tides around Taiwan,” in Advances in Engineering Mechanics – Reflection and Outlooks, In Honor of Theodore Y.-T. Wu, A.T. Chwang, M.H. Teng and D.T. Valentine, Eds, Singapore: World Scientific Publishing, 2005, pp.314-326.

[3] T. J. Simons, *Development of three-dimensional numerical models of the Great Lakes*, Sci. Ser., no 12, Canada Centre for Inland Waters, 1973, 26 pp.

[4] G. W. Platzman, *The dynamic prediction of wind tides on Lake Erie*, Meteor. Monog., vol.4, no. 26, Amer. Meteor. Soc., 1963, 44 pp.

[5] K. Matsumoto, T. Takanezawa and M. Ooe, “*Ocean tide models developed by assimilating TOPEX/POSEIDON altimeter data into hydrodynamical model: a global model and a regional model around Japan*,” Jour. Oceanog., vol. 56, no. 5, pp. 567-581, 2000.

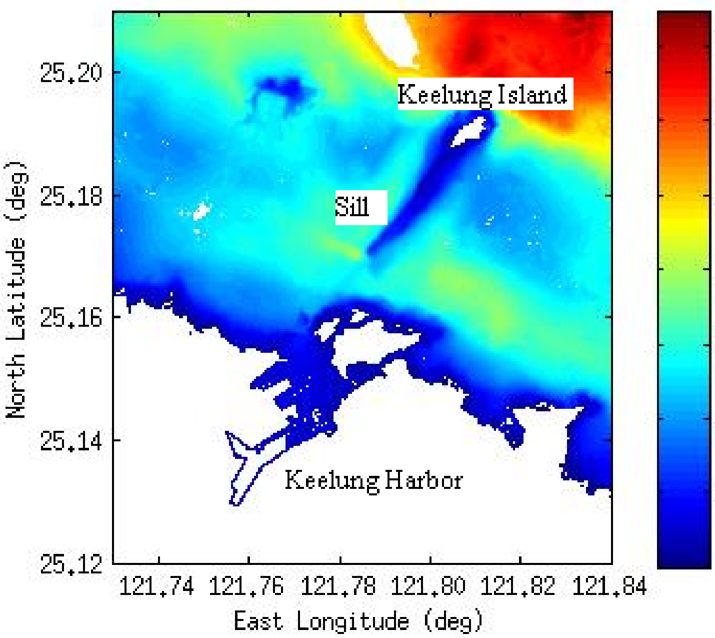

Figure 1. Bottom topography off Keelung harbor. The numbers by color bar denote depth in meters.

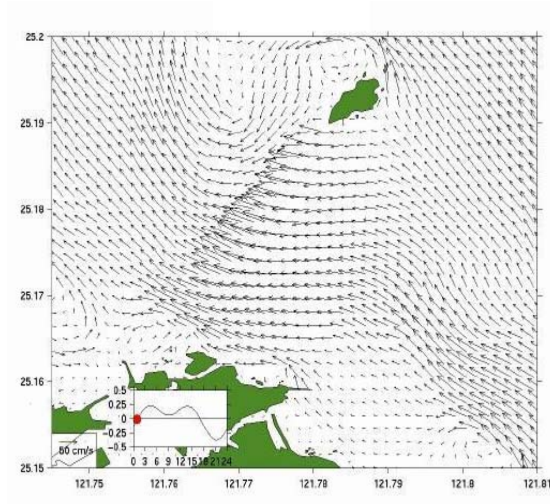

Figure 2. Simulation of tidal current distribution over Keelung Sill after 1-hr computation

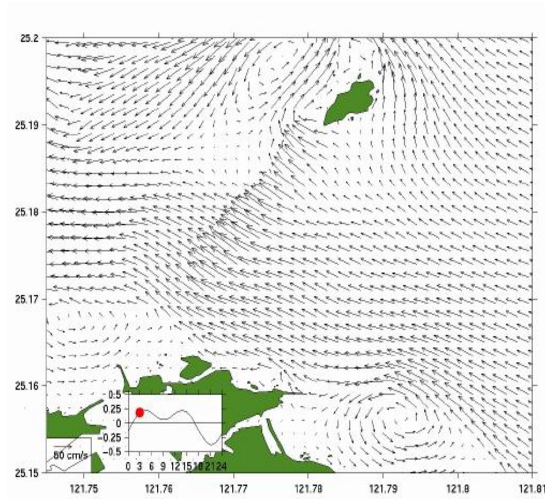

Figure 3. Simulation of tidal current distribution over Keelung Sill after 3-hr computation

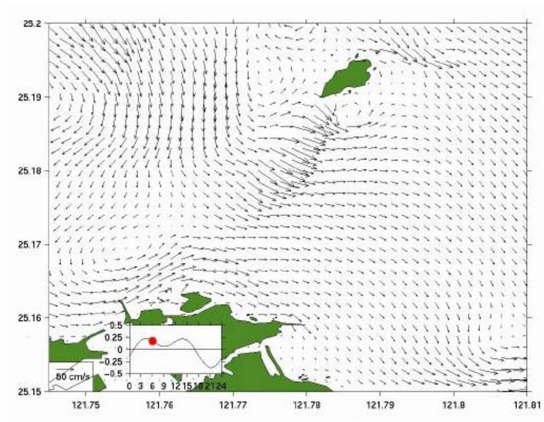

Figure 4. Simulation of tidal current distribution over Keelung Sill after 6-hr computation

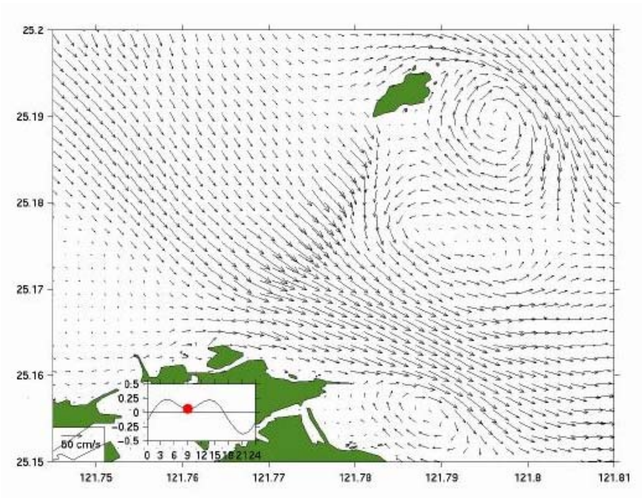

Figure 5. Simulation of tidal current distribution over Keelung Sill after 9-hr computation

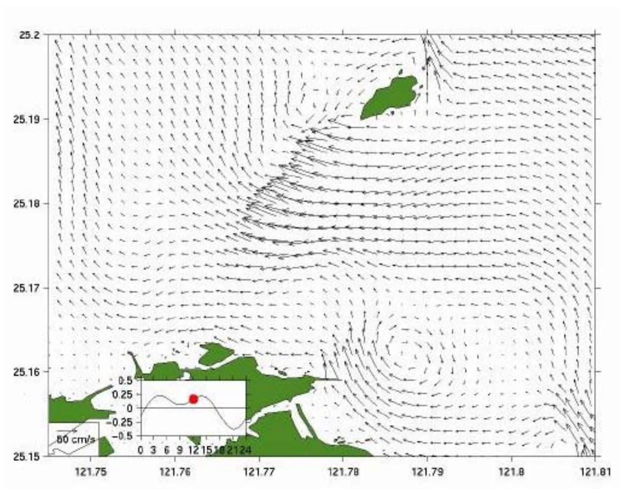

Figure 6. Simulation of tidal current distribution over Keelung Sill after 12-hr computation

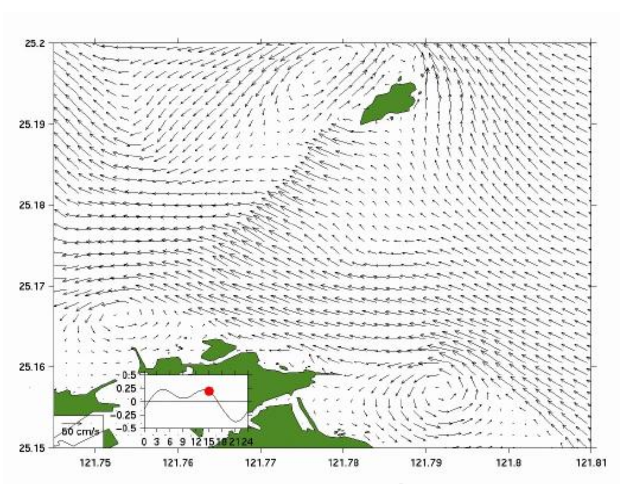

Figure 7. Simulation of tidal current distribution over Keelung Sill after 15-hr computation

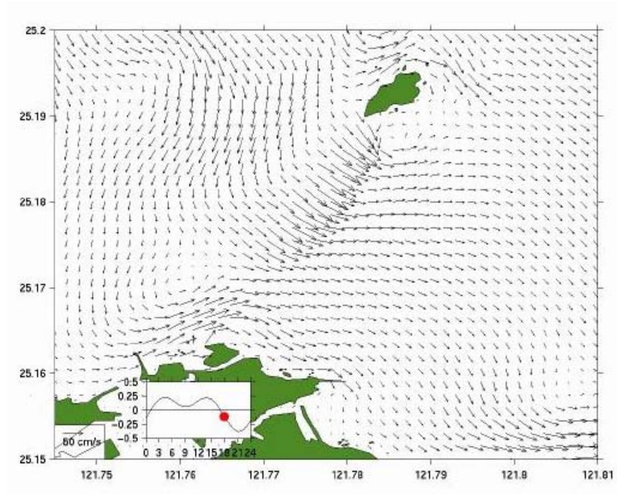

Figure 8. Simulation of tidal current distribution over Keelung Sill after 18-hr computation

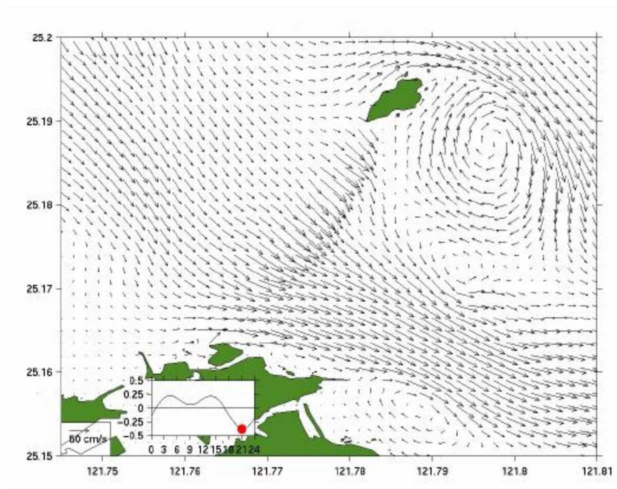

Figure 9. Simulation of tidal current distribution over Keelung Sill after 21-hr computation

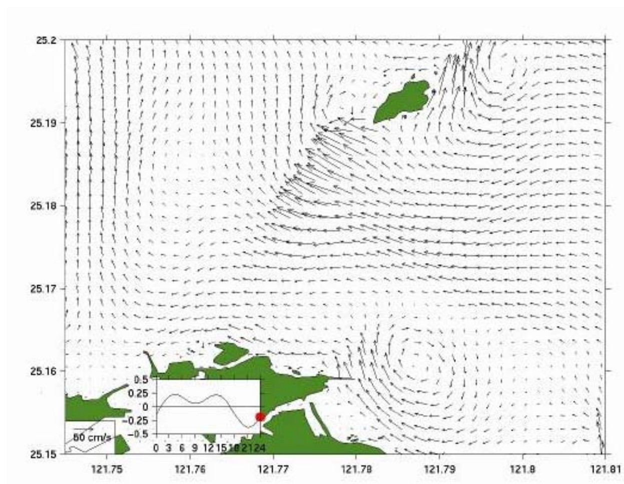

Figure 10. Simulation of tidal current distribution over Keelung Sill after 24-hr computation